PERGAMON

Quaternary Science Reviews 21 (2002) 837–851

QSR

Dry cave deposits and their palaeoenvironmental significance during the last 115 ka, Sodmein Cave, Red Sea Mountains, Egypt

J. Moeyersons[a,*], P.M. Vermeersch[b], P. Van Peer[b]

[a] *Royal Museum For Central Africa, B-3080 Tervuren, Belgium*

[b] *Laboratorium voor Prehistorie, Katholieke Universiteit Leuven, Redingenstraat, 16, B-3000 Leuven, Belgium*

Received in revised form 7 March 2000; accepted 10 July 2000

Abstract

The Sodmein cliff foot cave is the present-day remnant of an ancient cavity, probably of karstic origin. Physical breakdown of the limestone bedrock, rather than solution, has governed its subsequent evolution. Long before 115 ka BP an estimated 8000 m^3 of debris came off the weathered roof and mixed with contemporaneous cliff rockfall. Over 4 m of sediments have since accumulated. Wet conditions outside the cave during isotopic stage 5e are documented by sedimentary properties of the J-complex and by its detailed botanical and faunal content. These wet conditions were of regional significance. Shortly after 115 ka BP further subsidence of the roof of the ancient cave led to the present-day cave form. The cave interior has remained dry up to the present, but the deposits indicate an increase of animal passage and plant growth around 25 ka BP and during the Holocene interglacial. The latter period was rather arid in absolute terms, receiving less precipitation under a less regular pluvial regime, compared with the interglacial during isotopic stage 5e.

1. Introduction

The prehistoric site of Sodmein Cave (Prickett, 1979) in the Red Sea Mountains, Eastern Egypt (26°14′27″N, 33°58′12″E, Fig. 1), is currently under excavation (Vermeersch et al., 1994). The meteorological data from the nearest station, Quseir on the Red Sea coast, indicate hyperarid conditions. In the study area, 40 km further inland, some winter rains occur occasionally (Moeyersons et al., 1996, 1999). Humid conditions in the geological past are held responsible for karstic landscape modelling in several places in Egypt (Said and Issawi, 1964; El Aref et al., 1986). Sodmein Cave is the biggest known cavity in the Thebes limestone outcrops in the Gebel Um Hammad hogback. According to the latest TL-dates on burned chert fragments, the stratigraphical succession goes farther back than 115 ka BP (Mercier et al., 1999). This article provides evidence on the nature and age of these sediments in order of a better understanding of the Pleistocene climatic and environmental changes in this relatively unknown area.

*Corresponding author. Tel.: +32-2-769-5211; fax: +32-2-769-0242.

E-mail address: mrsons@africamuseum.be (J. Moeyersons).

2. General morphology

Sodmein Cave is developed in the lower part of a 100 m high cliff and looks over the 200 m wide wadi Sodmein at the downstream end of a 3 km long gap through the Gebel Umm Hammad, a hogback developed on Thebes Limestone of Eocene age (Vermeersch et al., 1994). The cave is located within a system of microfaults in the shoulder of a micrograben, traversing obliquely the gap (Fig. 2). The southern and northern side of the cave chamber coincide partly with faults and shear zones with vertical throw in the Thebes limestone of the order of 0.2–0.5 m.

The cavity (Fig. 3) starts deep in the Gebel with two subhorizontal shafts, both <1 m high. At about 35 m from their inferred outlet in the cliff, both tunnels end in the ceilings of a huge chamber with a steeply dipping backwall and an open view to the wadi (Fig. 4).

The southern shaft (Figs. 3 and 4) may be an old solution feature, having affected a 50 cm thick bedding layer in the Thebes limestone, about 0.5 m below the roof of the chamber. Several small hollows are visible in other parts of this layer which behaves as a cave inception horizon (Lowe, 1992). The roof of the southern shaft is crusted with a few calcite knobs and

0277-3791/02/$ - see front matter
PII: S0277-3791(01)00132-9

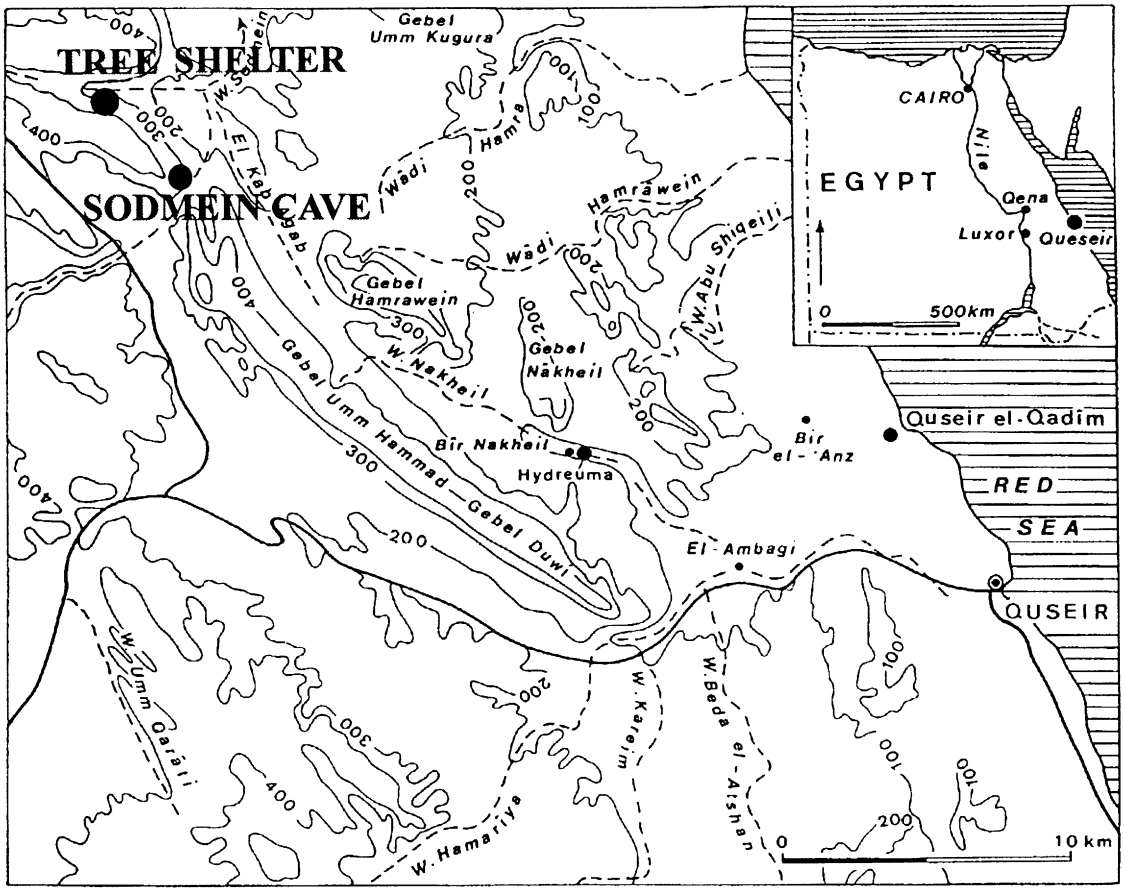

Fig. 1. Map of the study area.

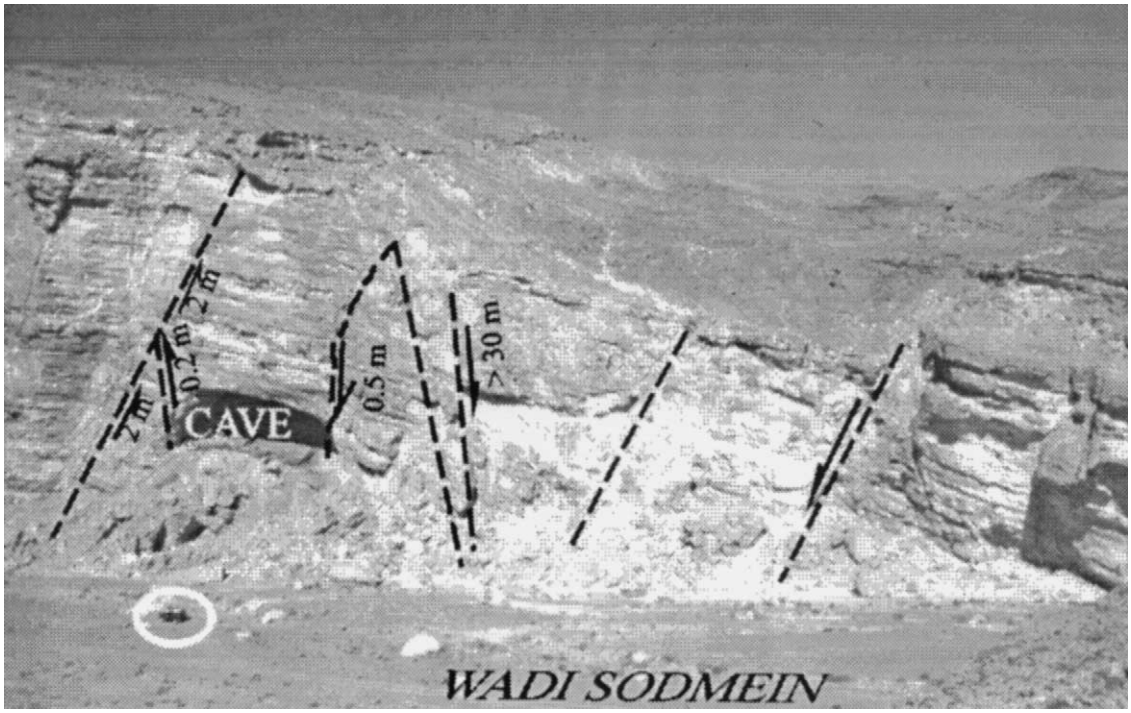

Fig. 2. Microtectonic setting of Sodmein Cave. Scale: see car in white circle.

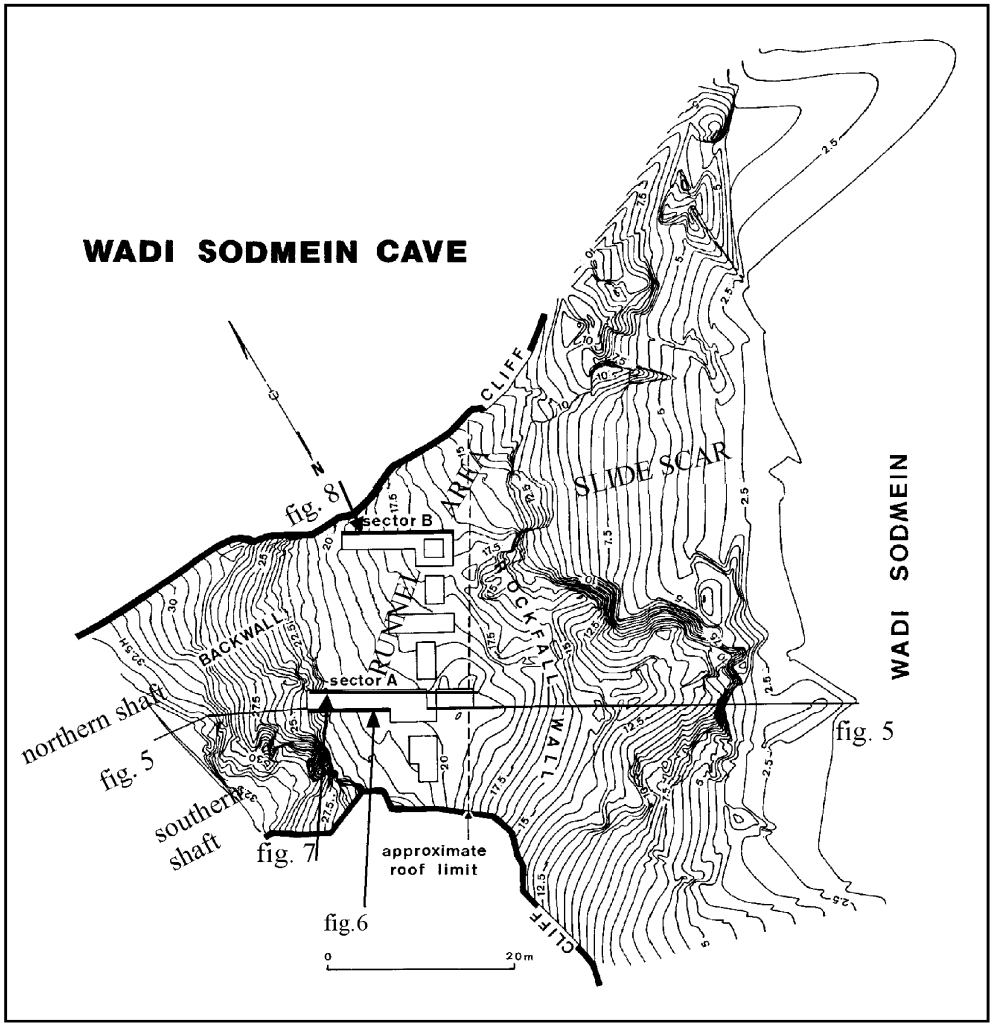

Fig. 3. Topographical map of Sodmein Cave. 10, 12.5, etc. are the relative heights in metres. Excavation pits are indicated.

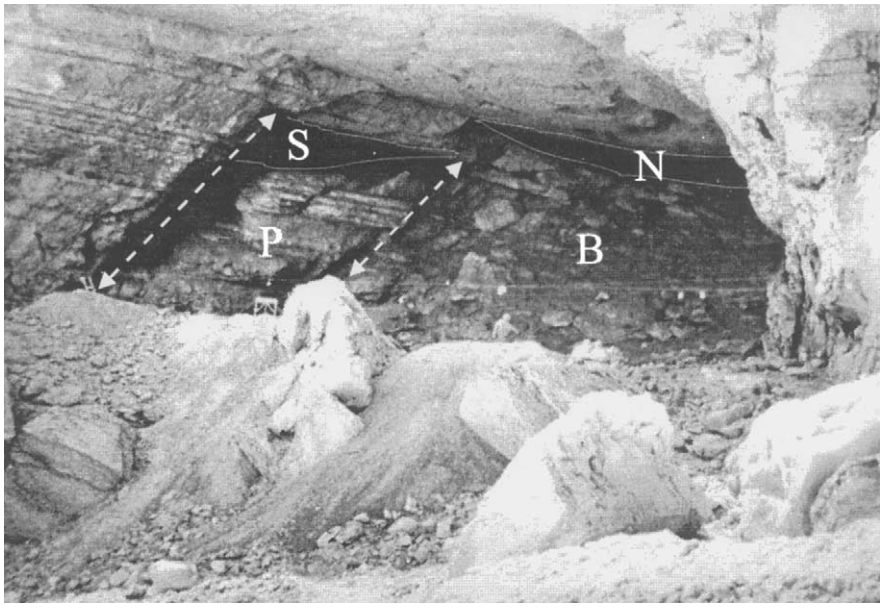

Fig. 4. Close view on Sodmein Cave: S, entrance of southern shaft; N, entrance of northern shaft; B, backwall; P, pillar-like promontory of the backwall between two joints in white dashes.

initial dripstones. The northern shaft is the collapsed part of the southern one.

The backwall (Fig. 5) of the cave consists of a subsided slab, which leans upon deposits in an underground cavity (Fig. 6). The sagging movement took place along the two vertical side joints of the cave (Fig. 2). The upper side of the slab shows a spongework of honeycomb weathering (Gill, 1981; Twidale, 1982; Uzun, 1998), interpreted as solutional features, a subcutaneous lapies (Baulig, 1966) due to important subsurface water infiltration in the bottom of the southern shaft before its collapse. The underside of the slab forms the ceiling of the subsurficial cavity and shows spheroidal weathering. This type of weathering occurs regularly in the Thebes limestone (Moeyersons et al., 1999). Corestones in the cave deposits are rounded, and bundles of flakes, being parts of their former spheroïdal weathering mantle, often adhere to their surface. The roof of the modern cave is flat and rather massive, apparently resulting from the mechanical detachment of a slab of rock. The cave floor in front of the backwall is a relatively flat and sandy area of $\pm 680\,m^2$, situated 15–21 m above the wadi.

A boulder field (Figs. 3 and 5) of Thebes limestone rock fragments with a minimum diameter of 1 m extends in front of the cave. Some huge rock masses are manifestly broken columns, which detached from the 90 m high cliff above the cave and either toppled or slid

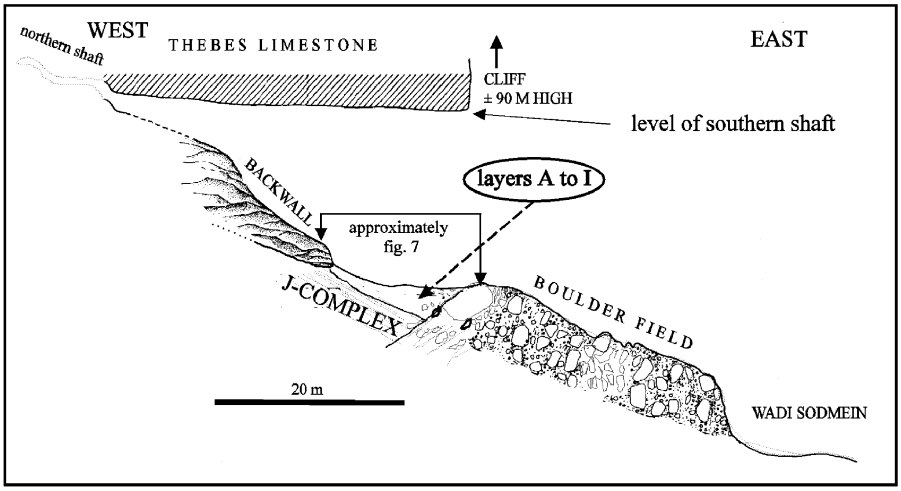

Fig. 5. Section through Sodmein Cave. Localisation on Fig. 3. The stratigraphy is schematically given. See Fig. 10 for previous cave evolution.

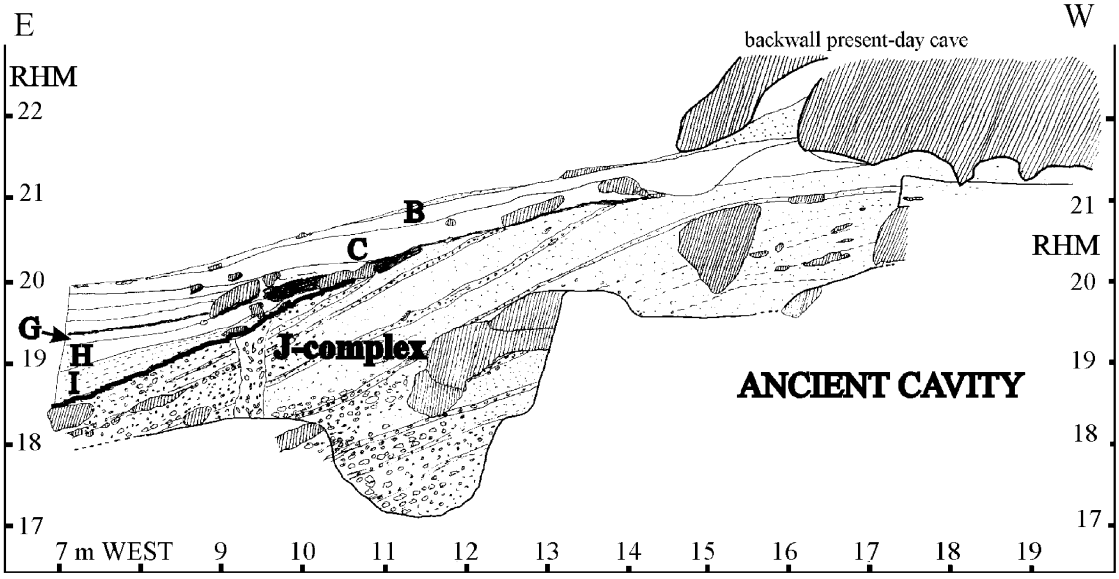

Fig. 6. Stratigraphical section along 21 m NORTH. B, C, etc. refer to the layers in Table 1. Rasters indicate Thebes limestone rock. Latitude WEST and EAST, longitude NORTH and relative height RHM (Figs. 6–8) are expressed in metres and refer to the excavation toponet. Localisation: see Fig. 3.

away from the cliff. The open structure between these very large limestone blocks, suggests a rapid collapse of the cliff in the past. Many open joints are still not filled up by the centimetres to decimetres sized rock rubble produced subsequently. The wadi Sodmein bed contains partly buried boulders which apparently slid or rolled into the river when the wadi bed was at least 2 m below its actual gravel aggradation level.

The top of the boulder field is located under the cliff and an equilibrium slope goes into the cave and to the wadi (Fig. 5). This situation is good evidence for its origin as cliff rockfall. However, the top of the inwards dipping part of the rockfall wall contains a few easily recognisable corestones, a few rock fragments with alveoli and typical chert bands as found in the inside of the cave. These rock fragments are found close to the entrance, and might, therefore, result from subsidence and fragmentation of the roof. An estimated 8000 m^3 of roof debris mixed with the boulder rockfall from the cliff.

The cliff rockfall boulder field and its inclusions of weathered rockfall from the roof of the buried cave extension are thus far the oldest known deposits at Sodmein. However, they must be much younger than the undergorund cave in which they fell. The rockfall deposits precede the development of other sediments, dipping towards the cave entrance and piled up behind the cliff rockfall. These deposits have been grouped as 'backfill' (Moeyersons et al., 1996) and comprise the J-complex and layers A–H, described below.

3. The cave deposits and their origins

The boulder field carries a discontinuous veneer of centimetre to decimetre sized rock clasts. This small rock rubble postdates the boulder field rockfall as it only partially fills the giant voids between the more than metre sized rock boulders. While the boulder cliff rockfall is clearly the result of cliff instability, possibly due to the incision of the Sodmein river bed far below its present-day aggradation level, the production of rubble is more likely to be related to small scale differential weathering of the Thebes limestone. In this respect, the free cliff faces as well as the free boulder faces and the free rock faces in the cave are to be considered as potential rubble source areas.

This rock rubble is more abundant on the boulder crest below the cliff, at least in sector A. Between the boulders it fills up at least 2–3 m thick pockets. The sections show that the rubble on the crest between the protruding big boulders is stratified and that this stratification, in spite of lateral intra-layer facies changes, can be prolongated into the so-called 'backfill' (Moeyersons et al., 1996) in the cave. This stratigraphical connection between the inside and the outside of the cave holds for the A–I layers. Fig. 8 shows how all these layers dip to the cave entrance but tend to bend over the boulder ridge. Subsequent erosion has, however, destroyed the accumulation there. The only 'backfill' deposits, in the sense of deposits retained behind the cliff rockfall are the deposits of the J-complex. As illustrated in Fig. 7, they die out against the boulder rockfall barrier, superficially filling the upper part of the open work structure between the boulders.

3.1. General description of the layers and their palaeoenvironmental significance

The cave deposits and their stratigraphy have been described elsewhere (Moeyersons et al., 1996). Table 1 summarises the stratigraphy, which has been subdivided from top to bottom:

- The A-layer: sand and small angular rockfall in the whole interior of the surface, thickness of the order of the 0.01–0.1 m.

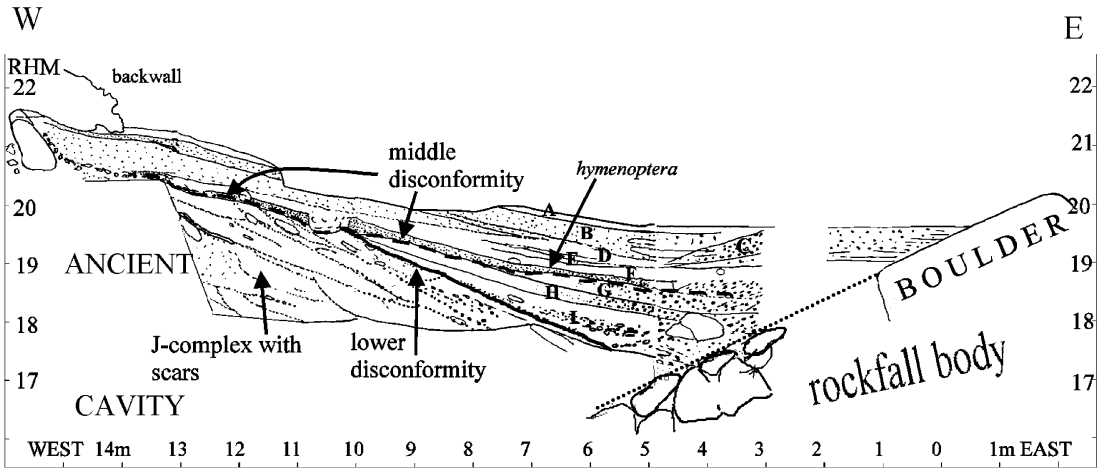

Fig. 7. Stratigraphical section along the line 23 m NORTH. Explanation see Fig. 6. Localisation: Figs 3 and 5.

- The layers B–I: rockfall rubble at the entrance, gradually changing into fine or at least finer grained 'backfill' further into the cave. Here, the succession contains dark layers B, D, F, G, I with organic contents rising to 36% of the weight. They alternate with whitish–yellowish layers C, E, H where in most cases the mineral component prevails. The dark layers contain a large spectrum of faunal and floristic organic remains. Most forthcoming are whole or mechanically broken animal droppings, but feathers, plant remains, seeds, small bones and insects also occur. Most organic material is in the same crumbled state as in the animal excrements and is therefore thought to have passed through the digestive system of animals. As mentioned earlier, the term 'backfill' might be somewhat misleading as it suggests sediments trapped behind other deposits. In fact, the three-dimensional configuration of the backfill is that of a large runnel, developed behind the cliff rockfall but flowing parallel to this barrier, in the direction of the northern cave wall.
- The J-complex: undergoes a lateral facies change cave inward. In the lower part it consists of rubble. Towards and below the backwall in the subsurficial cave extension it gradually becomes more sandy.

Table 1
Stratigraphy, dates and archaeological levels[a]

Layer	Archaeology	Dates
Superficial sand A		
Organic layer B	Neolithic	From ±6320
Whitish layer C	Occupations	To ±7470
Stratigraphical hiatus: geomorphological inactivity		
Organic layer D	UP1 and UP2	±25,200
Whitish layer E	MP 1	
Organic layer F	MP 2	
F/G disconf./layer	MP 3	⩾45,000
Organic layer G	MP 4	⩾30,000 and ⩾44,500
Whitish layer H		
Organic layer I		
Lower disconformity		
J-complex	MP 5	±115,000

[a]The age of the layers is further detailed on Table 2. The archeological levels are tentatively indicated: UP (Upper Palaeolithicum), MP (Middle Palaeolithicum).

At least three important disconformities can be distinguished. The upper one occurs somewhere at the base or within the A-layer. In Figs. 7 and 8, the B-layer is visibly interrupted or incised. It is not clear if this is due to natural erosion processes, driven for example by water leaking out of the ceilings, or the result of human perturbation. This nearly modern disconformity coincides with the erosion surface, which laterally cuts off the layers A–H in Fig. 8, and which appears to coincide with the actual topography in front of the cave.

The second disconformity separates the organic layers F and G in sector B (Fig. 8). This disconformity is characterised by the presence of a ±0.05 m thick layer of ground based hymenoptera nests. In sector A, this organic layer gradually develops into a sandy organic layer, several centimetres thick, and the F- and G-layer become parallel.

The lower disconformity is situated some 20–30 cm below the top of the rubble facies of the J-complex, but seems to be present only in the A sector.

The cave deposits excavated to date, are thought to have remained under very dry conditions since their deposition. This is suggested by a number of lines of evidence. First, there is the amazingly good preservation, in fact mummification, of floristic and faunal

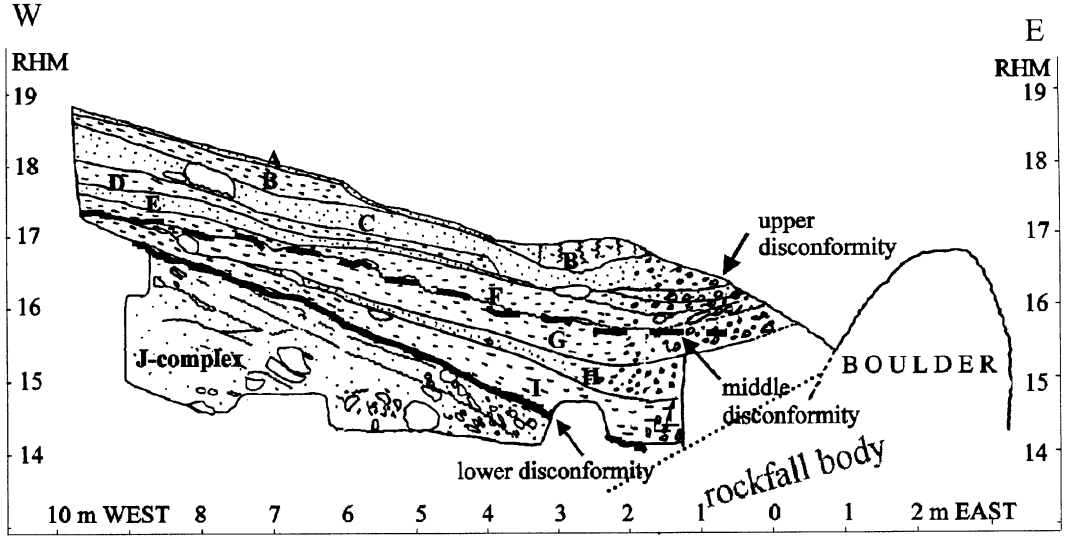

Fig. 8. Stratigraphical section along 40 m NORTH. Localisation of the section: see Fig. 3. Other explanations: see Fig. 6.

remains, indicating the absence of bacterial activity and fermentation in a humid soil environment. Second, secondary carbonate-cemented deposits are quasi absent inside the cave, but are well developed at the entrance and outside the cave. Wet augering in the cave showed that wetting of the deposits results in superficial cementation within 24 h. Repeated wetting in the past should have resulted in massive secondary carbonate crust formation. The extremely loose state of most of the deposits is significant in this context. Finally the >4 m thick succession of deposits, excavated, do not include a single level containing imbrication structures which would indicate deposition in flowing water. This suggests a dry cave environment, characterised by rock weathering processes like rock spalling by dust and salt activity, activated by dew water in joints, granular disintegration and flaking, and depositional and reworking processes like dry creep, gravitational grain flow, rockfall and eventually the mechanical action of passing man and animals. Local aeolian reworking of fines might explain the laminated structure of the finer, more organic beds and is believed to have also affected older layers (Section 3.3). The long term absence of water in the cave also excludes frost action there, even in the presence of frost-dew alternations. Therefore, the palaeoenvironmental value of the cave deposits resides not so much in the significance of in cave weathering and transport processes but in the faunal, floristic and anthropogenic inclusions, reflecting environmental conditions outside the cave.

3.2. Textural, morphoscopic and mineral characteristics of the deposits

In order to compare the textural composition of samples with a very variable gravel ($\geqslant$2000 μm) content, all granulometric curves have been calculated omitting the fraction above 2000 μm. Deposits are mostly bimodal but this bimodality is more weakly expressed in the layers below the middle disconformity. The coarse mode lies in the sand fractions $\geqslant$125 μm, the finer mode between 63 and 32 μm. The same phenomenon has been mentioned in the nearby Tree Shelter (Moeyersons et al., 1999). In Sodmein Cave, microscopic study showed that the coarse mode generally contains fresh looking and very angular (Powers, 1953) chert flakes, clearly resulting from mechanical breakdown, as well as Thebes limestone grains, often very irregular in shape, subangular to subrounded. The latter often show solution pits, and redeposited $CaCO_3$ has been observed, especially in joints, showing the role of crystal growth in splitting cherts as well as Thebes limestone fragments and in the production of flakes. This solution activity seems to be confirmed by the study of the silt mode in the bimodal samples. It contains for the very major part silt sized 63–2 μm (Kenney, 1984) quartz grains, generally transparent and very angular, combined with a lot of pieces of silicified and other non-solutional fragments of Thebes limestone fossils. A test (Moeyersons et al., 1999) of complete decalcification of a hand specimen of Thebes limestone showed that the 'decalcification loam' typically has the same content and size as the silt mode in the bimodal sediment type but does not show the coarse sand mode.

The bimodal character of the deposits H–I becomes less clear with depth, especially close to the cave entrance. In the J-complex, the granulometric curves are nearly rectilinear. Microscopic study shows that the sand fractions above 125 μm generally comprise a higher percent of chert flakes and grains than in the deposits above. In addition, the degree of chemical weathering of Thebes limestone debris is higher. On the other hand, the silt fractions below 63 μm contain not only the typical non-soluble residue, but also brown–yellow saccharoidal structures of secondary $CaCO_3$ precipitation. The post-depositional redistribution of $CaCO_3$ from the sand (2000–63 μm) into the silt (63–2 £m) (Kenney, 1984) explains the less pronounced bimodal character of the rockfall below the middle disconformity. Such redistribution is not in contradiction with the very dry cave environment, indicated above. Dew water is often held responsible for inter-grain calciumcarbonate migration and is present in the most arid places on earth (Goudie, 1989).

Gravel sized rock fragments (2×10^{-3}–2×10^{-2} m) have the same mineralogical and morphological characteristics as the sands. Above the middle disconformity, most debris is Thebes limestone flakes, probably mechanically destroyed old spheroidal weathering structures. Below the F/G transition and especially from the H-layer on, the chert debris outnumber the Thebes limestone flakes and clasts. In the J-complex nearly only chert occurs in the fractions above 2×10^{-3} m.

3.3. The J-complex backfill

The J-complex was first interpreted as dry rock- and dustfall (Moeyersons et al., 1996), supplied by the ceilings of the underground cavity and probably also, to a certain extent, by joints. The roof of the underground cave extension was an important source area because the J-complex comprises several corestones and weathered Thebes limstone blocks, embedded in a cave outward dipping stratigraphy. But the important chert content in the J-complex, being itself a dry deposit, might result from the collapse of a stock of material, inside the subsurficial cave extension, in which chert was overrepresented as a result of solution of limestone. The pre-J-complex 'wet' environment in the underground cavity is further documented by the presence, in the deepest

excavated J-complex levels, of cone-like and layered dripstones.

The rock- and dustfall interpretation needs some refinements in the case of sector A, to the West of the 9 m West line on Figs. 6 and 7. Here the material becomes very sandy, and the stratigraphical dip amounts to 42°. One explanation for such a steep slope is increased capillary cohesion in wet unsaturated fines: examples occur in talus (Hinchcliffe et al., 1998) and dune sands (Bigarella et al., 1969) are known. Further, the J-complex shows repeated cut and fill structures, small scale avalanching on the front slope of a cave outward growing sedimentary body. The scars of slump structures are known to preserve in damp sand conditions during deposition (McKee et al., 1971). In the arid environment of the Gebel Umm Hammad, steep sloping deposits with sand flow scars can be attributed either (1) to the lee slope of a dune, to (2) the stoss slope of a climbing dune (Evans, 1961) or to (3) a fan scree slope. The granulometric composition of the sand–loam fractions (Fig. 9) doesn't eliminate one of the possibilities. The lee dune hypothesis seems less probable, because it implies periodical strong airflow coming out of the fossil cave, but the possibility of a stoss slope of a climbing dune makes much sense. The talus scree hypothesis is not withheld here, because of the high probability that wet deposition should imply the occurrence of runoff, and hence formation of underground secondary carbonate-cemented deposits, which is not the case. Therefore, the J-complex in sector A is considered as a scree slope with part of the sand–loam fraction being reworked by slope-upward blowing wind during rain. During the process, limestone and chert debris of the order of 0.01–0.5 m have been furnished from the the inside of the relict cave.

The situation in sector B differs (Fig. 8). The mean dip slope is $<31°$ and avalanche scars are absent and in spite of the lower slope here, the actual stratigraphy doesn't match the criteria of pseudobedding (McKee, 1965) or climbing translatent stratification (Hunter, 1977). It appears, indeed, that the strata are too thick and too irregular in thickness (0.02–0.1 m), and that the stoney intercalations correspond to successive depositional surfaces, as tested by the presence of numerous

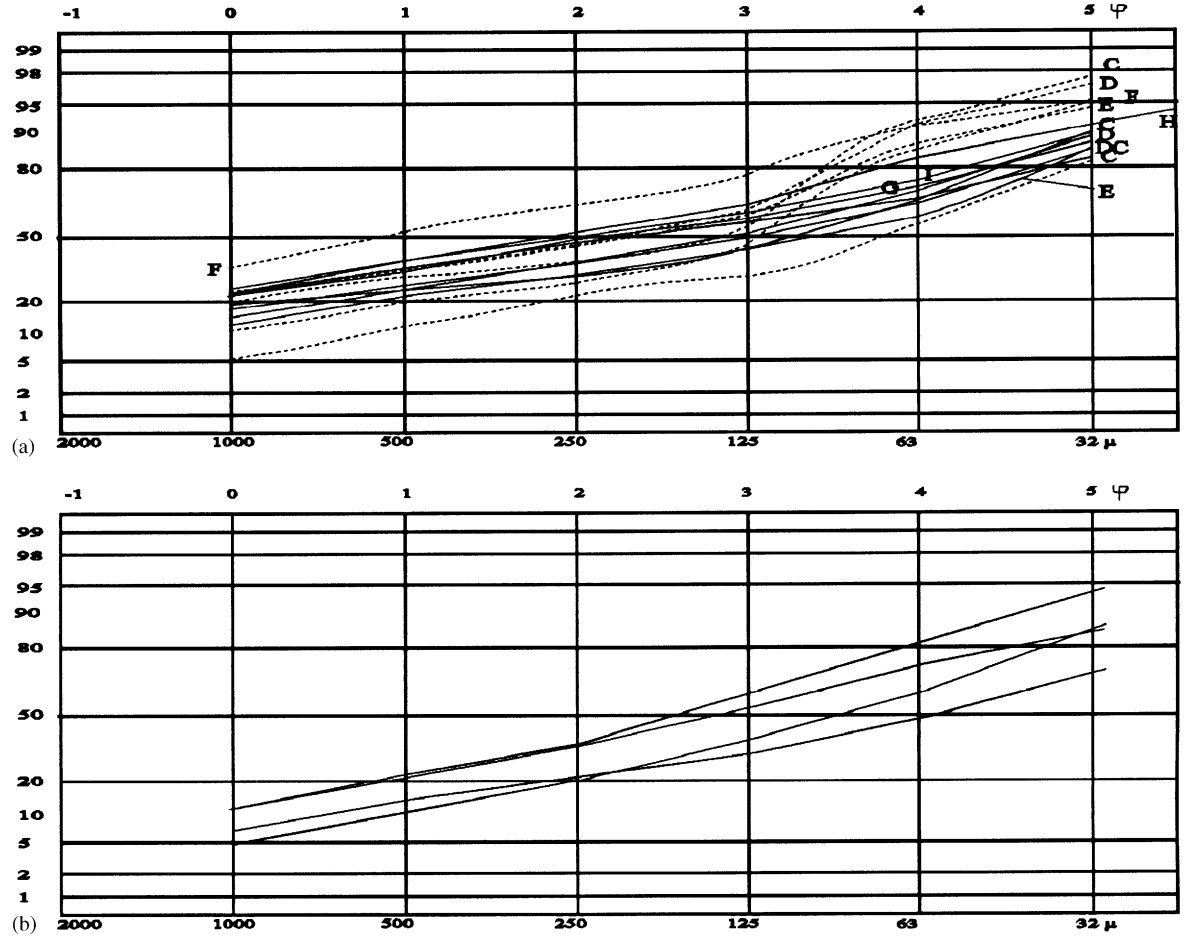

Fig. 9. (a) Textural composition of the rockfall rubble in the cave entrance. Bimodal texture type (dashes) is best expressed in samples from the upper layers. (b) Textural composition of the "sand" facies of the J-complex.

Table 2
Datations at Sodmein Cave and layers to which the dates refer

Date in yr BP	Lab. or author	Technique	Sector	Layer
6320±100	Lv-2082	^{14}C	a	Base of B-layer
6360±90	Lv-2085	^{14}C	A	Base of B-layer
6940±200	Lv-2083	^{14}C	A	Base of C-layer
7090±80	Lv-2086	^{14}C	B	C-layer
7350±80	Utc-3312	^{14}C	B	Base of C-layer
7470±110	Utc-3312	^{14}C	B	Base of C-layer
25,200±500	Utc-3313	^{14}C	B	Top D-layer
⩾45,000	Utc-3317	^{14}C	B	Disconf. F/G
⩾30,000	Lv-2084	^{14}C	A	G-layer
⩾44,500	Lv-2087	^{14}C	B	G-layer
±115,000	Mercier et al. (1999)	TL	A and B	Top J-complex

mats of plant relicts. Therefore, the facies of the J-complex in sector B is considered as the depositional area of sand flows. The stoney intercalations might result from the sandflow movements, known to push stones to the surface and to the edge of the flows (Pierson, 1980; Takalashi, 1981; Nieuwenhuijzen and Van Steijn, 1990; Bertran and Texier, 1994.).

3.4. The overlying cover

The A–C layers, described above, do not extend into the underground cavity but strike against the tip of the backwall. Their mineral component should, therefore, be supplied essentially by the ceilings of that part of the cave, visible today. This is confirmed by the less weathered state and generally angular form of the few bigger rock clasts, present, but also by the very low percentage of pure chert gravels (2×10^{-3}–2×10^{-2} m), compared with the J-complex, supplied from the inside of the underground cave extension.

On the basis of stratigraphy alone, the source of the D–I layers behind the rockfall ridge in the cave is less clear. The sections do not clearly indicate whether these layers came out of the subsurficial cave extension or were supplied by the backwall and shafts of the modern cave. But the A–I layers contain very similar material, in which large quantities of chert debris in the gravel and cobble fraction ($\geqslant0.002$ m) of the J-complex are lacking. Therefore, the present-day ceilings are considered as the source for the layers A–I, with some gravel beds in the latter being reworked J-complex material.

The change in supply between the J-complex and the layers above is explained by the forward sagging of the weathered slab in the back of the cave. Since the time the tip of the slab subsided, it leans on the wind reworked part of the J-complex and closures the entrance of the present-day underground cave extension. The order of subsidence of the slab at its tip is estimated at between 1 and 3 m.

3.5. The chronological framework

The chronology of vace evolution and palaeoenvironmental context is based on ^{14}C ages, supplemented by TL ages derived from lower deposits (Mercier et al., 1999). Table 2 presents the available data which are used in the development of the palaeoenvironmental history considered in the next section.

4. Cave history and palaeoenvironmental evolution

4.1. Undated events

The history of Sodmein Cave could be traced back to the existence of an old cavity. The situation is shown schematically on Fig. 10a. Not much is known about the dimensions of this old cliff foot recession, but it is likely that the cavity was laterally bound by the same subvertical joints which delimit the north and south side of the present-day cave. Its ceiling was about 10 m below the level of the present-day visible roof. The floor of the cave was probably at about the level of the actual wadi bed in front, but the question remains whether wadi Sodmein was already there or not. In the latter case, this old cave was an underground cavity with questionable access. But its roof was strongly weathered and showed solution hollows and spheroïdal weathering phenomena. Traces of a karstic seepage tunnel are still present on top of the remnant of this weathered roof. Broken drip stones and other debris of secondary limestone in the J-complex suggests a 'karstic' appearance of the relict cave, in an environment with higher calcite mobility than today. But conclusive evidence to suggest that the relict cave formed as the result of phreatic passage development (Gillieson, 1996) is lacking thus far.

Indirect evidence for the presence of wadi Sodmein in front of the cave comes from a later period, during which massive rockfall from the cliff in front of the

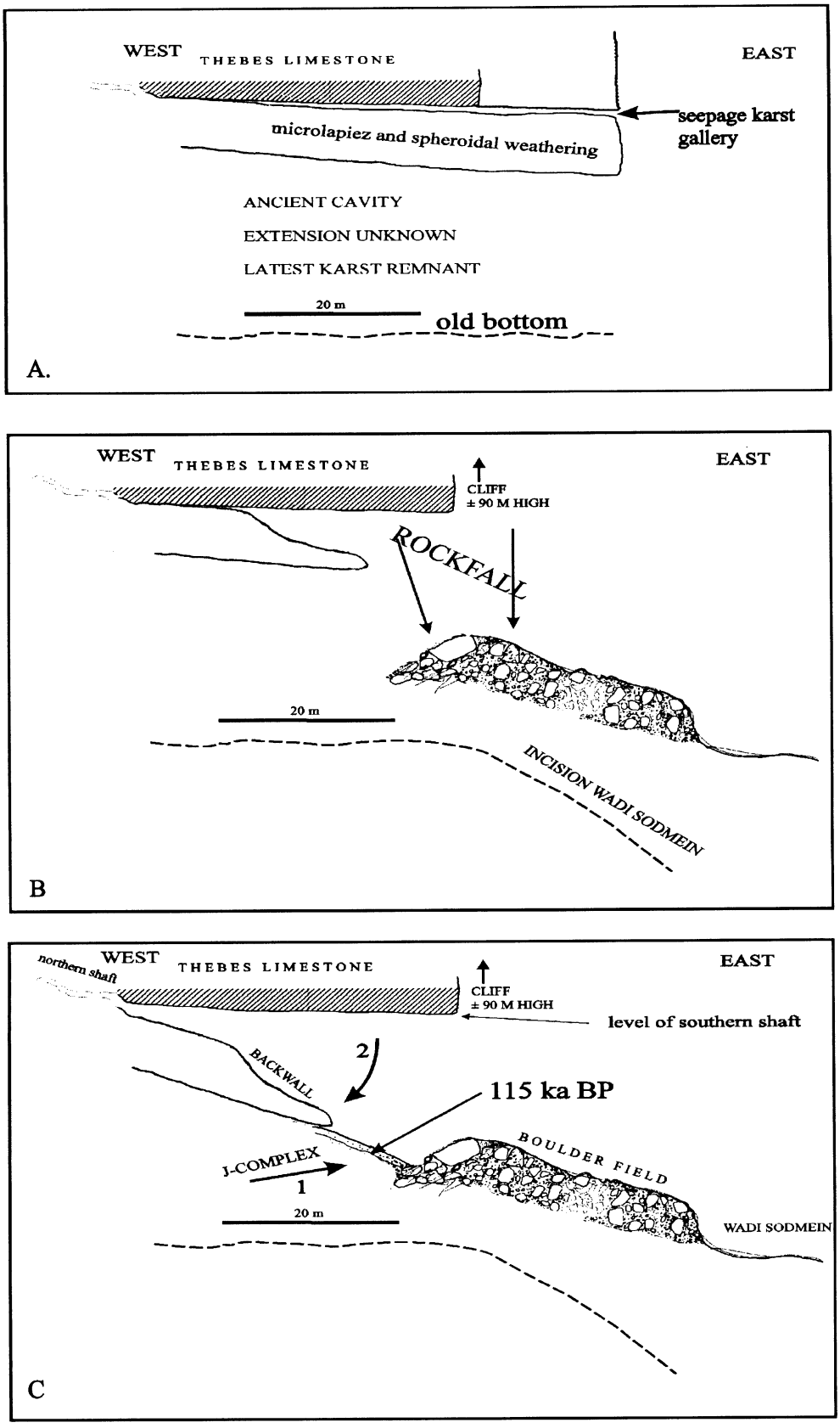

Fig. 10. Evolution of Sodmein Cave. Explanation see text.

ancient cave created a barrier at the entrance, the boulder field. Close to the entrance, part of the 10 m thick weathered slab in the roof came down during the same period. The situation is given in Fig. 10b. The high instability of the cliff is considered to be due to incision of the wadi Sodmein to several tens of metres below its actual aggradation bed. Much later, when secondary mass movements affected the boulder field, the wadi bed was still several metres below its actual level.

Close to, or during isotopic stage 5e, rockfall and rubble of the J-complex started to come out of the not-collapsed part of the ancient cave and formed a debris scree slope retained behind the boulder barrier.

4.2. Palaeoenvironmental evidence from the J-complex

In spite of the dry depositional context inside the cave, the J-complex contains abundant evidence for wet conditions outside the cave. Reworking and upslope blowing of the sand–loam fraction occurred probably during heavy rainstorms with northerly strong winds. There is also an abundant presence of humic material including plant micro-remains and feather partings. Soil samples contained one nearly intact insect, belonging to the order of *Diptera*, family of *Chironomidae*. Their immature stages occur in nearly every aquatic or wet habitat. Many species also inhabit soil, rich in organic matter, and adults often feed on honeydew. Furthermore, a big tree branch identified as *Ficus* sp. (*Moraceae*) and intact plant leafs belonging to different species occur as well. *Ficus* is an important genus, consisting of about 800 species, all from the tropics and the warm regions, especially Indo-Malaysia. The species could not be identified.

The J-complex contains also a lot of other plant remains, but only a small fraction could be determined. *Acacia tortilis* is certainly the tree most frequently used to make fire. Unburnt pieces of wood comprise: *Ficus* sp. (*Moraceae*), *Clematis* sp., *Balanites cfr. Aegyptiaca*, *Paliurus cfr. Spina Christi* (*Rhamnaceae*), *Brassicaceae*. Fragments of *Gramineae* and their typical phytoliths are abundant. Numerous leaf remnants point to the presence of foliages. The ensemble confirms conditions, much wetter than the actual desert.

Preliminary faunal analysis shows some remains of dorcas gazelle and rock dassie, but also a strong component of species associated with wetter environments. The latter comprise a large bovid (buffalo?), kudu and an elephantid. The existence of a local waterbody is attested by *Melanoides tuberculata*, which is a small, inedible gastropod typical of pools and swamps. Remains of crocodile and a catfish (*Clarias* sp.) indicate a former, at least temporary or intermittent, connection with the Nile basin, eventually followed by the subsistence of open, maybe isolated, water bodies. This connection implies at least a temporary regional extension of the wet conditions as recorded in the vicinity of the cave.

As mentioned above, the top of the J-complex has been TL-dated as $\pm 115{,}000$ BP (Mercier et al., 1999). This allows to attribute the evidence for a wet environment to the latest interglacial. Shortly after this date the slab in the backwall sagged and the deeper interior of the cave became closed. Therefore, no more deposits could leave the relict cave. This situation is depicted in Fig. 10c and shows that the ceilings of the modern chamber were the only cave source for the supply of the mineral component of layers A–I.

4.3. The layers A–I

The lower layers of this series, especially layer I, contain reworked material from the free lying slopes of the J-complex, enriched with flakes and sparse rockfall from the ceilings of the modern cave. This explains the local coarse open work structure of the I-layer and its high content of angular chert gravels in these places. Nevertheless, the bulk of the I-layer consists of organic material and therefore it belongs to the group of blackish layers.

The analysis and microscopic study of soil samples of the layers A–I deeper in the cave revealed that the whitish layers, just like the dark horizons, contain in the fractions below 0.002 m fragments of insects, teeth fragments of small rodents, fruit pellets, and other undefined organic material. The dark layers owe their colour to the abundant presence of sometimes slightly consolidated humate material, of animal faecal origin. In this way, the dark layers represent periods that vegetarian fauna visited the cave at regular times, while the whitish layers are periods during which the supply of mineral material from the ceilings has been much less contaminated by visiting fauna. The whitish layers are therefore considered to represent periods of reduced faunal populations.

Faunal remains from the upper organic B-layer comprise mainly ovicaprines (domestic sheep and goat), dorcas gazelle (*Gazella dorcas*) and rock dassie (*Procavia capensis*). The latter species has presently disappeared from the region as a result of extensive cutting of acacia trees. The environment, as reconstructed from the fauna, may have been comparable to, or slightly moister, than the present-day situation. The other organic layers D, F, G and I yield a mixture of species typically associated with desert or semi-desert and others presently living in dry, sparsely wooded savannas. The former group comprises dorcas gazelle, ibex (*Capra ibex*) and barbary sheep (*Ammotragus lervia*). The latter group consists of species presently having a more southerly distribution such as wild ass (*Equus africanus*), Soemmering's gazelle (*Gazella soemmeringi*), greater kudu (*Tragelaphus strepsiceros*), vervet monkey

(*Cercopithecus* cf. *aethiops*), hunting dog (*Lycaon pictus*), serval or caracal (*Felis* sp.), and leopard (*Panthera pardus*).

The plant remains in the organic B-layer show a high diversity with *Cadaba Farinosa* Forsk, *Acacia cfr. tortilis* (Forsk.) Hayne, *Salvadora Persica* L. and at least 6 other undefined plants. The whitish C-layer contains large quantities of *Tamarix* sp. and *Olea* sp. The latter might point to general wet conditions but it might also indicate the presence of an oasis in the vicinity, like Bir Nakheil today (Fig. 1). In the blackish D-layer, several different woods are present, one of them being *Boscia senegalensis* (Pers.) Lam. ex Poir., an arbust from the Sahel. Further, *Salvadorica Persica* L., *Caparis decidua* and *Ziziphus* sp. are present. Especially in the G- and I-layers, grass phytoliths regularly occur and shell fragments are present. In the whitish H-layer, *Tamarix* sp., *Acacia* sp., *Nitraria* sp. and *Pistacea* sp. could be determined.

The combined faunal and floristic inventory shows that the dark layers reflect wetter environments than today with a rather high faunal and floristic diversity. The degree of humidity seems to grow from young to old, culminating in the I-layer, which should represent wet conditions, maybe approaching the ones found in the J-complex.

The whitish layers may represent periods of environmental degradation, relative to forgoing and following wetter pulses, but they certainly do not represent hyperarid conditions like today or during the last glacial maximum. A good example is the whitish upper backfill C-layer. It contains a lot of fruit fragments and undefined pellets, charcoal, one calcified sprig and secondary $CaCO_3$, showing the presence of plant life and water in the area. The ages of charcoal from hearths in the C-layer (Table 2) rank along the wet period between two still wetter pulsations, respectively, at ± 8000 and ± 6600 yr BP (Moeyersons et al., 1999).

4.4. Local and regional comparisons

The dates from the B- and C-layers are nicely time-clustered. The C-layer is estimated to have been formed within a time span of $< \pm 900$ yr.

The time gap between the base of the C- and the top of the D-layer coïncides with the last maximum of the Würm glaciation and the first Holocene millenia in Europe. The absence in North-East Africa of deposits dating from the LGM is not unusual. Many interfluvial locations underwent deflation or other erosion processes (Paulissen and Vermeersch, 1987; Wendorf et al., 1989; Brookes, 1993, just to mention a few). The absence in Sodmein Cave of mineral deposits or of a stratigraphical disconfomity from the period ± 7500–25,000 yr BP indicates that the cave ceiling and the deeper gallery walls did not produce rock debris or dust. The entrance and the inside of the cave were geomorphologically inactive (Rohdenburg, 1970). However, in the river valley environment of Wadi Kubbaniya in Southern Egypt, this dry period saw impressive overbank alluviation by an anastomosing river with reduced discharge (Wendorf et al., 1989).

In Sodmein Cave the dry conditions in the vicinity are indicated by the absence of organic deposits from this period, suggesting no passage of animals during that period.

The D-layer, from before this period, again indicates wetter conditions before and around $\pm 25{,}000$ yr BP and apparently corresponds with a wet period recorded in several parts in Africa and South-West Arabia: between 28 and 24 ka BP in the Eastern Sahara (Pachur et al., 1990); the humid pulsation between 35 and 24 ka BP in Eastern Africa (Voigt et al., 1990); the wetter episode at the Lake Chad between 28 and 22 ka BP (Durand, 1982); in northern Mali where the wet period ended around 21 ka BP (Petit-Maire, 1989); in the Nile valley between 21/22 and 25 ka BP (Paulissen and Vermeersch, 1987); in the Ethiopian rift lakes from 30 to 21 ka BP (Gasse et al., 1980) and further in the Horn of Africa (Voigt et al., 1990); in the crater lake Barombi Mbo and in the West Cameroonese forests between 28 and 20 ka BP (Maley and Brenac, 1998; Maley, 1991), roughly between 30 and 20 ka BP on the western escarpment of the volcanic line in Cameroon (Moeyersons, 1997); in Sub-Saharan Africa around 30 ka BP (Grove and Warren, 1968; Faure, 1969; Rognon and Williams, 1971; Rognon, 1976; Street and Grove, 1976; Sonntag et al., 1980); in the Southwestern Arabian lakes (McClure, 1976; Hötzl and Zötl, 1979); sapropels near the Nile mouth, deposited around 30 ka BP (Stanley and Moldano, 1977).

No definite ^{14}C-dates are available below the D-layer and the middle disconformity and the F/G-layer equivalent in the southern part of Sodmein Cave is already older than 45,000 y BP.

The oldest date in Sodmein, the 115 ka BP TL-date, comes from the top of the J-complex. It dates the last moment of contact between chert debris and fire (Mercier et al., 1999). According to the age of 115 ka BP, it seems logical to consider the wet period represented by the J-complex as the African wet equivalent of the Eemian interglacial. This wet period centers around 125–130 ka BP in the palaeolake Shati in central Lybia (Petit-Maire et al., 1995). The grey lake beds of Bir Tarfawi in the Eastern Sahara have the same age (Wendorf et al., 1987) and the authors claim that the Eastern Sahara received at that time maybe as much as 600 mm precipitation per annum and that the groundwater level was high.

Other humid pulses have been distinguished in the region. Still in the Eastern Sahara, a humid pulse at 90 ka BP has been identified in the so-called olive-green

silts (Wendorf et al., 1987). In the palaeolake Shati, wet pulsations are found at 90 and 77 ka BP (Petit-Maire et al., 1995). In Northern Somalia, the Eemian equivalent and the two subsequent humid pulses are, respectively, dated at 138, 108, and 78–70 ka BP (Voigt et al., 1990). Some evidence for another and more recent wet period between 45 and 40 ka BP comes from Southern Egypt (Szabo et al., 1989; McHugh et al., 1988). This corresponds with the 46–41 ka old wet pulsation in northern Mali (Morel et al., 1991), and with the 40 ka old humid period at palaeolake Shati (Petit-Maire, 1982). In Wadi Kubbaniya, a dry period has been determined between ±45 and ±60 ka BP, but no evidence for a subsequent wet pulsation is mentioned (Wendorf et al., 1989).

Table 3 correlates the Sodmein stratigraphy with the known wet periods in Northern Africa. It is stressed here that thus far only three wet periods have been dated in Sodmein Cave: a part of the Holocene, roughly between 6300 and 7500 yr BP, a wet period around 25,000 yr BP and the wet period of isotopic stage 5 at 115 ka BP. A complete and really reliable correlation will only be possible after dating the F-, G- and J-layers.

Table 3
Firmly established correlations between the Sodmein Cave layers and known or supposed wet periods in Africa below the equator[a]

Wet periods in Africa north of the equator		Stratigraphy Sodmein
		A-layer
Early Holocene wet period "interglacial"		B-layer, C-layer
		Stratigraphical hiatus
25–30 ka BP wet pulsation		D-layer
±40 ka BP wet pulsation	NO CORRELATION	F-layer
±77 ka BP wet pulsation	NO CORRELATION	To
±90 ka BP wet pulsation	NO CORRELATION	I-layer
±125 ka BP: Eem "interglacial" wet		J-complex

[a] The wet periods are referred to in the text.

5. Conclusions

5.1. Sodmein Cave and karst

The above preliminary description of the origin and evolution of Sodmein Cave (Fig. 10) shows that real karst activity with the ability to create solution caves, could have occurred prior to isotope stage 5e. From 115 ka BP on, several episodes of environmental conditions wetter than today have occurred. They include the subactual Holocene and the last Pleistocene interglacial. But even during these relatively wet periods, physical breakdown of the Thebes limestone, either by fragmentation into debris and flakes or disintegration into sand–loam seems to have been much more important than limestone solution and correlative redeposition. Regional evidence for ancient karst activities in the form of secondary $CaCO_3$ formations like travertines has never been found in the Nakheil valley and surroundings. Maybe much of this type of evidence is buried in the river gorges deep below the present-day levels of the aggraded wadi beds.

5.2. Comparison between the Holocene and the last Pleistocene interglacial

In this paper, evidence has been presented for wet periods in the area occupied by Sodmein Cave at 6320–7470 and ±25,000 yr BP and at ±115 ka BP. Other wet periods, not yet dated, occurred between the two latter dates. The terms 'humid' or 'wet', used here, point to the relative idea of wetter conditions than the present-day hyperarid ones. But, in absolute terms, 'wet' and 'humid' may cover a very wide range of conditions. To illustrate this, comparison is made between the isotopic stage 5e interglacial and the Holocene (Table 4).

The first is rather well documented in Sodmein (Section 4.2). Rainstorms fed a network of more or less permanent water bodies, linked to the Nile. Big animals populate an acacia tree savannah with a grass

Table 4
Precipitation regime, fauna and flora during the Holocene and isotopic stage 5e interglacials

Interglacials	
Holocene (6–8 ka BP)	Isotopic stage 5e (at 115 ka BP)
Sparse rains and maybe oasis in vicinity	Rainstorms giving rise to permanent pools, swamps (*Melanoides tuberculata*) and other water bodies with crocodile and a catfish (*Clarias* sp.).
About ten tree species, but the present-day *Acacia cfr. Tortilis* (Forsk.) Hayne, and *Tamarix* sp. Prevail	Acacia three savannah with *Balanites cfr. Aegyptiaca* and *grasses. Ficus* sp. (*Moraceae*), *Clematis* sp. (*Ranunculaceae*) and several foliages in wetter spots
Present-day desert fauna with dorcas gazelle (*Gazella dorcas*) and rock dassie (*Procavia capensis*).	Big savannah fauna with bovids (buffalo?), kudu and an elephantid
Domestic sheep and goat	
Hymenoptera, and other insects	Flies (*chironomidae*)
Rodents	

understorey and insects were present. The occurrence of other trees like *Ficus* sp. (*Moraceae*), *Clematis* sp., *Balanites cfr. Aegyptiaca*, *Paliurus cfr. Spina Christi* (*Rhamnaceae*), *Brassicaceae* confirm savannah-like conditions.

This certainly does not represent a desert environment and an annual precipitation of 600 mm, suggested for the wet period around 125 ka BP in the Eastern Sahara (Wendorf et al., 1987; Wendorf et al., 1993) would also be conceivable at Sodmein.

As to the Holocene, it is represented in Sodmein by layers A–C and by a faunal and floristic diversity, indicating somewhat wetter conditions than at present, but without exotic elements typical of wetter environments to the South or North. The impression exists that the Sodmein environment during the Holocene was only slightly less arid, similar to the Tree Shelter only a few km away from Sodmein (Moeyersons et al., 1999). Also Kröpelin (1989), when defining 'humidity' in the Gilf Kebir area in South-western Egypt, claims that the Holocene 'wet' period between 8200 and 6100 y BP contains only 70 depositional events, which suggests a rain-induced flow event every 30 yr. The flow events must have been rather severe as they caused local ponding during some weeks or maybe months. The idea of severe rains with a multidecennial recurrence has been confirmed for the Tree Shelter and might also hold in the case of the Sodmein Cave, but here the problem is to know the percentage of the total number of rains causing a flow event in the cave entrance. The 'somewhat drier' C-layer, covering a period of ± 800 yr, contains about 15 calcified laminae shown in the right part of Fig. 7 at the entrance of the cave. This means one flow event every 53 yr, or about 2 large rainfall events a century similar to what Kröpelin (1989) suggests for the drier periods. At the Tree Shelter, rains during the period considered are known to be rather moderate and no information exists as to the percentage of rainstorms which caused flow events in the past. A conservative speculation that only one percent of the forthcoming rains may have caused a flow event in the cave entrance, suggests an average of about two rains per 'rainy season'. This remains indicative for dry, arid conditions and we consider part of the 'wet' early and middle Holocene, and the 'wet' periods represented in Sodmein by the D- and F-layers as periods of rather arid climate in absolute terms. It is thought that the wet lower part of the Holocene interglacial in Egypt, compared with the Eemian interglacial, received less precipitation under a less regular precipitation regime.

Acknowledgements

This research project is funded by the 'Fonds voor Wetenschappelijk Onderzoek-Vlaanderen' and the 'Onderzoeksfonds K.U. Leuven'. We thank H. Beeckman, E. De Coninck, H. Doutrelepont and W. Van Neer, Royal Museum for Central Africa (Tervuren, Belgium) for the palaeobotanical, palaeoentomological and palaeofaunal determinations.

References

Baulig, H., 1966. Vocabulaire franco-anglo-allemand de géomorphologie. Les Belles Lettres, Paris, 230pp.

Bertran, P., Texier, J.-P., 1994. Structures sédimentaires d'un cône de flots de débris (Vars, Alpes Françaises Méridionales). Permafrost and Periglacial Processes 5, 155–170.

Bigarella, J.J., Becker, R.D., Duarte, G.M., 1969. Coastal dune structures from Parana (Brazil). Marine Geology 7, 5–55.

Brookes, I.A., 1993. Geomorphology and Quaternary geology of the Dakhla Oasis Region, Egypt. Quaternary Science Reviews 12, 529–552.

Durand, A., 1982. Oscillations of Lake Chad over the past 50 000 yr: new data and new hypothesis. Palaeogeography, Palaeoclimatology, Palaeoecology 39, 37–53.

El Aref, M.M., Awaldalah, F., Ahmed, S., 1986. Karst landform development and related sediments in the Miocene rocks of the Red Sea coastal zone, Egypt. Geologische Rundschau 75, 781–790.

Evans, J.R., 1961. Falling and climbing sand dunes in the Cronese ("Cat") Mountain area, San Bernadino County, California. Journal of Geology 70, 107–113.

Faure, J., 1969. Lacs quaternaires du Sahara. Mitteilungen der Internationale Vereinigung für Limnologie 17, 131–146.

Gasse, F., Rognon, P., Street, F.A., 1980. Quaternary history of the Afar and the Ethiopian rift lakes. In: Williams, M.A.J., Faure, H. (Eds.), The Sahara and the Nile. Balkema, Rotterdam, pp. 361–489.

Gill, E.D., 1981. Rapid honeycomb weathering (tafoni formation) in greywacke, S.E. Australia. Earth Surface Processes and Landforms 6, 81–83.

Gillieson, D., 1996. Caves: Processes, Development and Management. Blackwell, Cambridge, 324pp.

Goudie, A.S., 1989. Weathering processes. In: Thomas, D.S.G. (Ed.), Arid Zone Geomorphology. Belhaven Press, London, pp. 11–24.

Grove, A.T., Warren, A., 1968. Quaternary landforms and climate on the south side of the Sahara. Geographical Journal 134, 194–208.

Hinchcliffe, S., Ballentyne, C.K., Walden, J., 1998. The structure and sedimentology of relict talus, Trotternish, Northern Skye, Scotland. Earth Surface Processes and Landforms 23, 545–560.

Hötzl, H., Zötl, J.G., 1979. Climatic change during the Quaternary period. In: AlSayari, S.S., Zötl, J.G. (Eds.), Quaternary Period in Saudi Arabia. Springer, New York, pp. 301–311.

Hunter, R.E., 1977. Basic types of stratification in small eolian dunes. Sedimentology 24, 361–387.

Kenney, C., 1984. Properties and behaviours of soils relevant to slope instability. In: Brunsden, D., Prior, D.B. (Eds.), Slope Instability. Wiley, Chichester, pp. 27–65.

Kröpelin, S., 1989. Untersuchungen zum Sedimentationsmilieu von Playas im Gilf Kebir. In: Kuper, R. (Ed.), Forschungen zur Umweltgeschichte der Ostsahara. Heinrich-Barth-Institut, Köln, pp. 183–306.

Lowe, D.J., 1992. A historical review of concepts of speleogenesis. Cave Science 19, 63–90.

Maley, J., 1991. The African rain forest vegetation and palaeoenvironments during late Quaternary. Climatic change 19, 79–98.

Maley, J., Brenac, P., 1998. Vegetation dynamics, palaeoenvironments and climatic changes in the forests of western Cameroon during the

last 28,000 years B.P. Review of Palaeobotany and Palynology 99, 157–187.
McClure, H.A., 1976. Radiocarbon chronology of Late Quaternary lakes in the Arabian Desert. Nature 263, 755–756.
McHugh, W.P., Cauley, J.F., Haynes, C.V., Breed, C.S., Schaber, G.G., 1988. Palaeorivers and geoarchaeology in the southern Egyptian Sahara. Geoarchaeology 3, 1–40.
McKee, E.D., 1965. Experiments on ripple lamination. In: Middleton, G.V. (Ed.), Sedimentary Structures and their Hydrodynamic Interpretation, Vol. 12. Special Publications of the Society of Economic Paleontology and Mineralogy, Tulsa, pp. 66–83.
McKee, E.D., Douglas, J.R., Rittenhouse, S., 1971. Deformation of leeside laminae in eolian dunes. Geological Society of American Bulletin 82, 359–378.
Mercier, N., Valladas, H., Froget, L., Joron, J-L., Vermeersch, P.M., Van Peer, P., Moeyersons, J., 1999. Thermoluminescence dating of a middle-palaeolithic occupation at Sodmein Cave, Red Sea Mountains. Egyptian Journal of Archeological Sciences 26, 1139–1345.
Moeyersons, J., 1997. Geomorphological processes and their palaeoenvironmental significance at Shum Laka cave (Bamenda, western Cameroon). Palaeogeography, Palaeoclimatology, Palaeoecology 133, University of Zimbabwe Publications, Harare 103–116.
Moeyersons, J., Vermeersch, P., Van Peer, P., Van Neer, W., Beeckman, H., De Coninck, E., 1996. Sodmein Cave site, Red Sea Mountains, Egypt: development, stratigraphy and palaeoenvironment. In: Pwiti, G., Soper, R. (Eds.), Aspects of African Archaeology. Papers from the 10th Congress of the Panafrican Association for Prehistory and Related Studies, Harare, pp. 53–62.
Moeyersons, J., Vermeersch, P.M., Beeckman, H., Van Peer, Ph., 1999. Holocene environmental changes in the Gebel Umm Hammad, Eastern Desert, Egypt. Geomorphology 26, 297–312.
Morel, A., Tillet, Th., Poupeau, G., 1991. Le bassin de Taoudenni. In: Tillet, G. (Ed.), Palaeoenvironments and Prehistoric Populations of the Sahara in the Upper Pleistocene. Abstracts Colloque de Solignac (PICG 252).
Nieuwenhuijzen, M.E., Van Steijn, H., 1990. Alpine debris flows and their sedimentary properties. A case study from the French Alps. Permafrost and periglacial processes 1, 111–128.
Pachur, H.J., Kröpelin, S., Hoelzman, P., Goshin, H., Altmann, H., 1990. Late quaternary fluviolacustrine environments of western Nubia, Sudan. Berliner Geowissenschaftlicher Abhandlungen 120, 203–260.
Paulissen, E., Vermeersch, P.M., 1987. Earth, man and climate in the Egyptian Nile valley during the Pleistocene. In: Close, A.E. (Ed.), Prehistory of Arid North Africa. Southern Methodist University Press, Dallas, pp. 29–67.
Petit-Maire, N., 1982. Le Shati, lac pléistocène du Fezzan (Lybie). CNRS, Marseille.
Petit-Maire, N., 1989. Interglacial environments in presently hyperarid Sahara: palaeoclimatic implications. In: Leinen, M. (Ed.), Modern and past patterns of global atmospheric transport. Kluwer, Dordrecht, pp. 637–661.
Petit-Maire, N., Sanlaville, P., Yan, Z., 1995. Oscillations de la limite nord du domaine des moussons africaine, indienne et asiatique, au cours du dernier cycle climatique. Bulletin de la Société géologique de France 166, 213–220.
Pierson, T.C., 1980. Erosion and deposition by debris flows at Mt Thomas, North Canterbury, New Zealand. Earth Surface Processes 5, 227–247.
Powers, M.C., 1953. A new roundness scale for sedimentary particles. Journal of Sedimentary Petrology 23, 117–119.
Prickett, M., 1979. Quseir regional survey. In: Whitcomb, D.S., Johnson, J.H. (Eds.), Quseir Al-qadim 1978 Preliminary Report. Cairo-American Research Center in Egypt, Cairo, pp. 257–349.
Rognon, P., 1976. Oscillations climatiques au Sahara depuis 40 000 ans. Revue de géographie physique et de géologie dynamique 18, 147–282.
Rognon, P., Williams, M.A.J., 1971. Late Quaternary climatic changes in Australia and North Africa: a preliminary interpretation. Palaeogeography, Palaeoclimatology, Palaeoecology 21, 285–327.
Rohdenburg, H., 1970. Morphodynamische Aktivitäts- und Stabilitätszeiten statt Pluvial- und interpluvialzeiten. Eiszeitalter und Gegenwart 21, 81–96.
Said, R., Issawi, B., 1964. Geology of northern plateau, Bahariya Oasis, Egypt, Vol. 29. Geological Survey of Egypt, Cairo.
Sonntag, C., Thorweihe, U., Rudolph, J., Lohnert, E.P., Junghans, C., Munnich, K., Klitzsch, E., El Shazly, E., &Swailem, F., 1980. Isotopic identification of Saharan groundwaters, groundwater formation in the past. In: Van Zinderen Bakker, E.M. (Ed.), Palaeoecology of Africa, 12. Balkema, Rotterdam, pp. 158–171.
Stanley, D.J., Moldano, A., 1977. Nile cone: late quaternary stratigraphy and sediment dispersal. Nature 266, 129–135.
Street, A.F., Grove, A.T., 1976. Environmental and climatic implications of late Quaternary lake level fluctuations in Africa. Nature 261, 385–390.
Szabo, B.J., McHugh, W.P., Schaber, G.G., Haines, C.V., Breed, C.S., 1989. Uranium-series dated authigenic carbonates and Acheulian sites in southern Egypt. Science 243, 1053–1056.
Takalashi, T., 1981. Debris flow. Annual Review of Fluid Mechanics 13, 57–77.
Twidale, C.R., 1982. Granite Landforms. Elsevier, Amsterdam.
Uzun, A., 1998. Weathering forms on sandstones directly exposed to sea effects in Gelincikburnu and its surroundings (south coast of the Black Sea). Zeitschrift füer Geomorphologie Neue Folge 42, 233–244.
Vermeersch, P.M., Van Peer, P., Moeyersons, J., Van Neer, W., 1994. Sodmein Cave site, Red Sea Mountains (Egypt). Sahara 6, 31–40.
Voigt, B., Gabriel, B., Lassonczy, K., Ghod, M., 1990. Quaternary events at the Horn of Africa. Berliner geowissenschaftliche Abhandlungen 120, 679–694.
Wendorf, F., Close, A., Schild, R., 1987. Middle Palaeolithic occupations at Bir Tarfawi, Egypt. African Archaeological Review 5, 4963.
Wendorf, F., Schild, R., Close, A.E., 1989. The prehistory of Wadi Kubbaniyavol. 2: stratigraphy, paleoeconomy and environment. Southern Methodist University Press, Dallas.
Wendorf, F., Schild, R., Close, A., Associates, 1993. Egypt during the last interglacial: the middle palaeolithic of Bir Tarfawi and Bir Sahara East. Plenum Press, New York, London.